

# Mach-Zehnder and Michelson topologies for self-referencing fiber optic intensity sensors

**José M. Baptista, MEMBER SPIE**

Instituto Superior de Engenharia do Porto  
Rua S. Tomé  
4200 Porto, Portugal

and

INESC Porto  
Unidade de Optoelectrónica e Sistemas  
Electrónicos  
Rua do Campo Alegre 687  
4169-007 Porto, Portugal

**José L. Santos, MEMBER SPIE**

Universidade do Porto  
Dep. de Física  
Faculdade de Ciências  
Rua do Campo Alegre 687  
4169-007 Porto, Portugal  
and  
INESC Porto  
Unidade de Optoelectrónica e Sistemas  
Electrónicos  
Rua do Campo Alegre 687  
4169-007 Porto, Portugal  
E-mail: jlsantos@goe.fc.up.pt

**Armindo S. Lage, MEMBER SPIE**

Universidade do Porto  
Dep. de Engenharia Electrotécnica e de  
Computadores  
Faculdade de Engenharia  
Rua dos Bragas  
4099 Porto Codex, Portugal

**Abstract.** A theoretical and experimental study of self-referencing fiber optic intensity sensors based on Michelson and on Mach-Zehnder configurations is conducted. Via the definition of the measurement parameter  $R$ , sensor linearity and sensitivity are analyzed. Theoretical and experimental results are compared, considering the problem of sensor design and optimization. The choice between the two configurations is addressed; the Michelson one is recommended for practical reasons.  
© 2000 Society of Photo-Optical Instrumentation Engineers. [S0091-3286(00)03406-1]

Subject terms: optical fibers; optical sensors; optical fiber sensors; optical fiber intensity sensors.

Paper 980473 received Dec. 22, 1998; revised manuscript received Dec. 8, 1999;  
accepted for publication Dec. 9, 1999.

## 1 Introduction

Optical fiber intensity-modulated sensors are very attractive in that they are simple in concept, reliable, and small and offer a wide range of applications at lower cost.<sup>1</sup> However, to ensure accurate measurements with such sensors, the implementation of a reference channel is vital. Such a channel will provide insensitivity to source intensity fluctuations and to variable transmission losses of the fiber link and connectors, which are often indistinguishable from transducer-caused effects.<sup>2</sup>

The implementation of a certain referencing technique depends in general on the specific transduction mechanisms in order to eliminate the effects of unwanted modulation. There are several ways to implement a reference channel. Most reported techniques use one of the following encoding mechanisms: time-of-flight difference,<sup>3</sup> wavelength encoding,<sup>4</sup> or frequency response.<sup>5</sup>

The use of the interfering concept as the basis of a self-referencing intensity-type sensor has already been mentioned in the literature, in an approach that is known as amplitude-phase conversion.<sup>6,7</sup> In it, the optical power injected into the system is sine-wave-modulated. In the sens-

ing head, a fraction of that power is not affected by the measurand, constituting a reference signal that, when combined with the other fraction that was intensity-modulated by the measurand, gives a resulting optical-power intensity sine wave, with a phase (relative to the phase of the electrical signal that modulates the optical power emitted by the optical source) dependent only on the optical loss induced in the sensor head by the measurand (apart from a constant factor determined by the length of the lead/return fiber). The evaluation of this relative phase allows information to be obtained about the measurand status independently of the optical power fluctuations that can occur outside the sensor head.

We have developed another frequency-based approach to have a self-referencing intensity-type optical fiber sensor.<sup>8,9</sup> It relies on the degree of constructive interference between the intensity sine waves generated in the sensing cavity when it is illuminated by light from an optical source with its intensity modulated at different frequencies. For a fixed cavity length this degree of constructive interference is only dependent on the sine-wave frequency. Therefore, if on reception one takes the ratio of the amplitudes of the

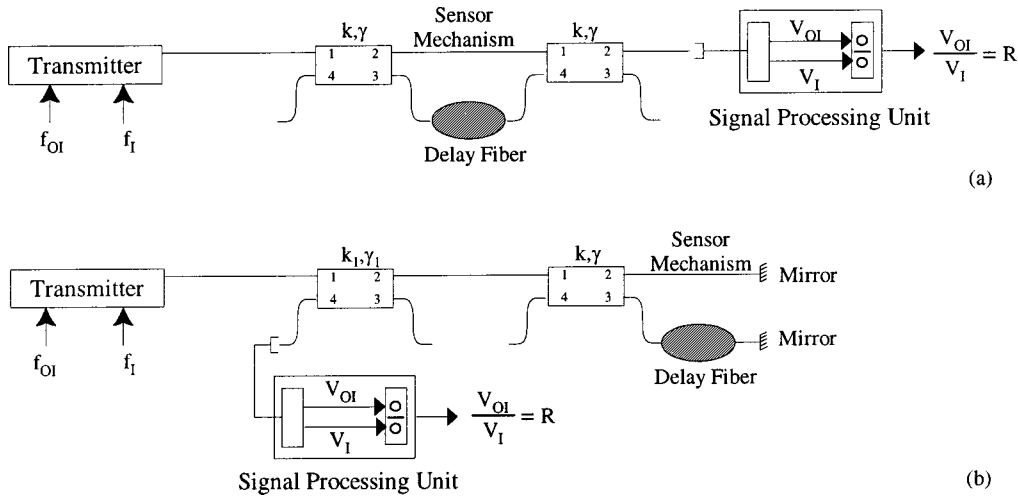


**Fig. 1** Block diagram of the sensing structures: (a) Mach-Zehnder; (b) Michelson.  $V_{OI}$  and  $V_I$  are voltages proportional to the amplitudes of the output optical power sinewave waveforms at an off-constructive-interference frequency ( $f_{OI}$ ) and at a constructive interference frequency ( $f_I$ ), respectively.

signals corresponding to the interference of two or more waveforms arriving from the sensing cavity and obtained when the intensity of the optical source is modulated at two different frequencies, then the result only depends on the losses induced by the measurand in the sensor head in all or in some of those waveforms, independent of any other optical losses that can occur in the rest of the optical system. In the present work this concept is developed further, and the performance of interferometric intensity sensors based on Mach-Zehnder and Michelson sensing-head configurations is evaluated in detail.

We begin by characterizing the transfer function for each of the two topologies. Then we define the measurement parameter in order to analyze the linearity and sensitivity of the sensors. A comparison of their characteristics for different realizations of those configurations is also presented. Finally, the results are compared, addressing the features of the better of the two configurations here proposed.

## 2 Sensor Concept

The proposed sensor concepts are illustrated in Fig. 1. The frequency response of a Mach-Zehnder or Michelson configuration when the optical power input comes from an optical source intensity modulated at a particular frequency shows that for some frequencies the amplitude of the output optical power waveform is maximum (constructively interfering frequencies), while for other frequencies it results in a decreased output optical power (off-constructively interfering frequencies). Therefore, the intensity modulation at different frequencies of the light injected into these fiber structures provides different amplitudes for the output optical power waveforms via the above-mentioned transfer functions. The ratio between two of these amplitudes, one obtained at a frequency where off-constructive interference occurs and another obtained in constructive interference, depends on the light modulation induced inside the fiber

sensing interferometers and is free from light-source fluctuations and variable transmission losses that can occur outside those structures.

Of the proposed schemes, the Michelson topology [Fig. 1(b)] allows the sensing part of this structure to be located remotely and apart from the signal processing. For this configuration, it is not necessary to install another segment of fiber from the sensing part to the signal processing, as it would be for the Mach-Zehnder topology [Fig. 1(a)].

Figure 2 illustrates the frequency response of the Mach-Zehnder [Fig. 2(a)] and Michelson [Fig. 2(b)] configurations subject to losses. These functions emerge from the theoretical analysis given in the next section. The parameter  $g$  is the attenuation factor externally induced in the fiber structures. For  $g=1$ , there is no induced loss and the amplitude of the modulated output light is maximum, while for  $g=0$  the light in one arm of the interferometer is completely lost. For both topologies, we can see that when the value of the induced losses rises, in other words when  $g$  gets closer to zero, the distance between the peaks and the valleys shortens until the graph becomes a horizontal line. On the other hand, when there are no external losses induced in the fiber interferometers ( $g=1$ ), the distances between the peaks and the valleys are at their maximum, being dependent only on the internal losses of those fiber structures (losses in fiber, splices, couplers, etc.).

Comparing the two graphs shown in Fig. 2, for equal values of the induced loss (equal  $g$  in both cases) the shape of the transfer function is more squeezed in the Michelson configuration than in the Mach-Zehnder. This happens because, the Michelson topology being a reflective one, the light passes twice through the structure and therefore experiences the applied induced loss twice before reaching the detector, in contrast with the Mach-Zehnder topology, where light passes only once through the fiber structure before reaching the detector.

As indicated above, the ratio of the value of the transfer function at an off-constructive-interference frequency to its

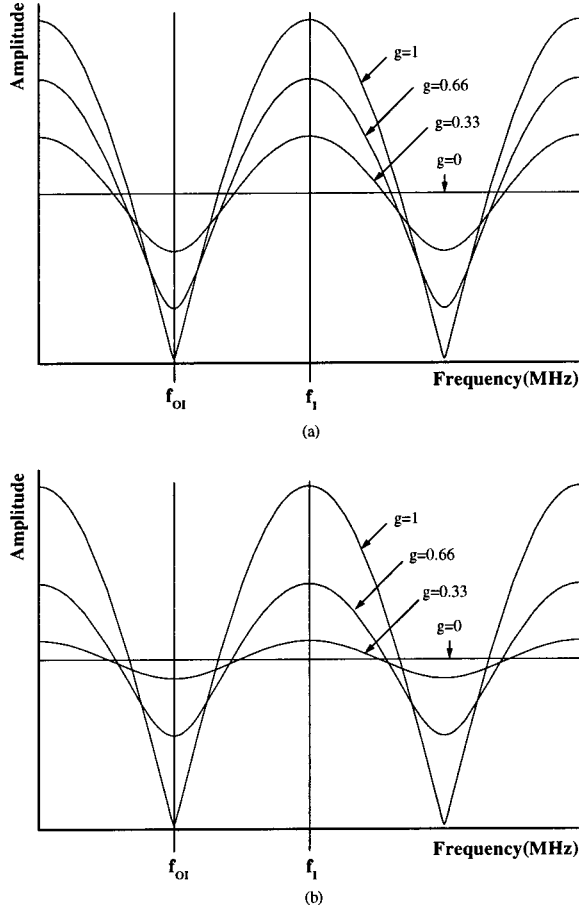


**Fig. 2** Transfer function of (a) Mach-Zehnder and (b) Michelson topology with the induced loss factor  $g$  as a parameter. The ordinate is the amplitude of the output optical power waveform as a function of frequency.

value at a constructive-interference frequency depends only on the optical losses inside the fiber sensing structure (intrinsic and induced losses), and not on optical power fluctuations induced outside the sensor head. Therefore, the modulation of that ratio ensures a self-referencing scheme that makes the measurand readout independent of possible unwanted light intensity modulation along the optical system.

The operation principle of the intensity sensor studied in this work is based on the concept described above when applied to the Mach-Zehnder and Michelson sensing-head configurations.

### 3 Theoretical Analysis

The analysis presented in this section addresses the Mach-Zehnder and the Michelson configuration. In what follows it will be assumed that the intrinsic losses of these sensing structures can be neglected.

#### 3.1 Transfer Function

For both cases shown in Figs. 1(a) and 1(b), if the injection current of the optical source is modulated at angular frequency  $\omega$  via a voltage signal of the form

$$V_{\text{in}} = A \cos \omega t, \quad (1)$$

then in the Mach-Zehnder configuration the output optical power reaching the detector generates a proportional voltage signal given by

$$V_{\text{out}} = T_1 A \beta \Psi_{\text{MZ}} \cos \omega t + T_2 A \beta \Psi_{\text{MZ}} \cos(\omega t + \phi), \quad (2)$$

while for the case of the Michelson structure it is given by

$$V_{\text{out}} = T_3 A \beta \Psi_{\text{MI}} \cos \omega t + T_4 A \beta \Psi_{\text{MI}} \cos(\omega t + 2\phi). \quad (3)$$

In both cases dc levels have been ignored,  $\beta$  is a factor that represents the conversion of the electrical input voltage waveform into a corresponding optical power waveform emitted by the optical source and the conversion of the detected optical power into a proportional output voltage signal, and  $\Psi_{\text{MZ}}$  and  $\Psi_{\text{MI}}$  are factors that take account of the optical losses induced into the lead and return fibers for the Mach-Zehnder and Michelson configurations, respectively. Also,

$$T_1 = (1 - \gamma)^2 (1 - k)^2,$$

$$T_2 = (1 - \gamma)^2 k^2 g,$$

$$T_3 = (1 - \gamma)^2 (1 - \gamma_1)^2 (1 - k_1) k_1 (1 - k)^2 r_1,$$

$$T_4 = (1 - \gamma)^2 (1 - \gamma_1)^2 (1 - k_1) k_1 k^2 g^2 r_2,$$

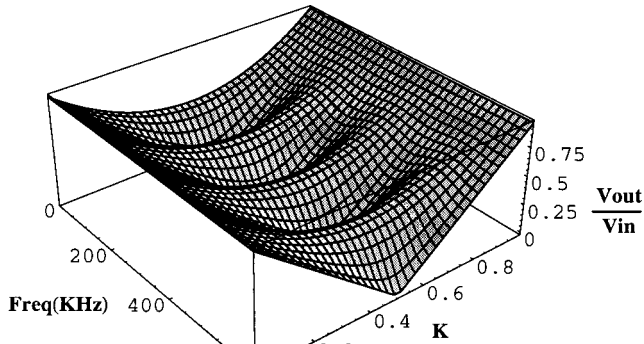
$$\phi = 2\pi \frac{nfL}{c},$$

where  $A$  is the amplitude of the modulating input voltage wave,  $\gamma$  and  $k$  are, respectively, the excess loss factor and the coupling coefficient of the couplers in the sensing structures (Fig. 1),  $\gamma_1$  and  $k_1$  are the excess loss factor and the coupling coefficient of the input coupler in the Michelson topology ( $k_1 = 0.5$ ),  $g$  is the induced loss factor in the sensing heads,  $n$  is the refractive index of the fiber,  $f$  is the modulating frequency ( $\omega = 2\pi f$ ),  $L$  is the path difference between the two arms in the Mach-Zehnder and in the Michelson configuration,  $\phi$  is the static phase difference between the two interfering intensity waves,  $c$  is the velocity of the light in vacuum, and  $r_1$  and  $r_2$  are the reflectivities at the ends of ports 2 and 3 of the Michelson coupler, respectively. In this analysis it was decided to consider the same coupler parameters ( $k, \gamma$ ) for those couplers that integrate the sensing structures, and different parameters for any other couplers that eventually need to be used in the fiber system (for example, parameters  $k_1$  and  $\gamma_1$  for the branching coupler in the Michelson topology).

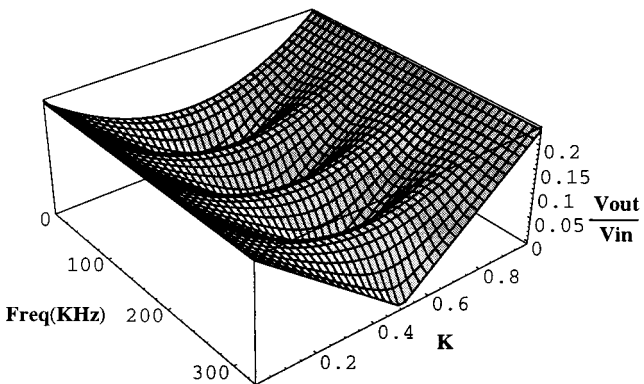
Defining the system transfer function as the ratio between the output voltage and input voltage signals, we have for the Mach-Zehnder structure

$$\frac{V_{\text{out}}}{V_{\text{in}}} = \beta \Psi_{\text{MZ}} (T_1^2 + T_2^2 + 2T_1 T_2 \cos \phi)^{1/2}, \quad (4)$$

and for the Michelson structure



(a)



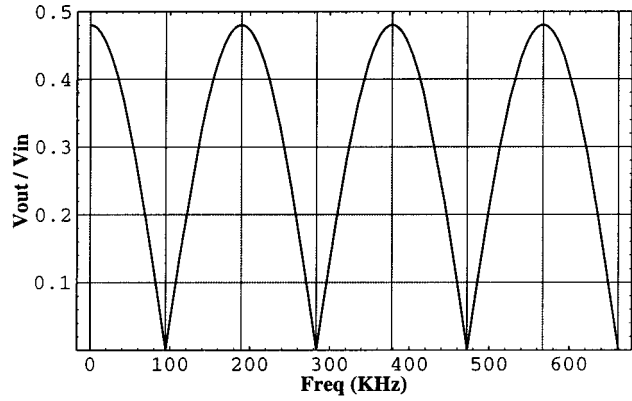
(b)

**Fig. 3** Transfer functions for the Mach-Zehnder (a) and Michelson (b) configurations (it is assumed that no losses are induced in the fiber resonators, i.e.,  $g=1$ ).

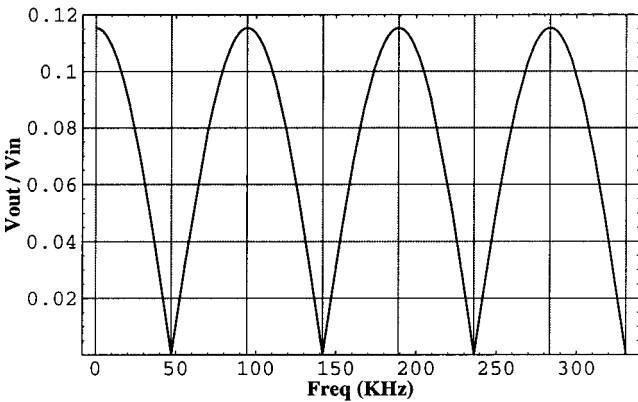
$$\frac{V_{\text{out}}}{V_{\text{in}}} = \beta \Psi_M (T_3^2 + T_4^2 + 2T_3 T_4 \cos 2\phi)^{1/2}. \quad (5)$$

These equations give the transfer functions of the Mach-Zehnder and Michelson configurations, respectively, in their dependence on the modulating frequency and the coupling coefficient of the sensing-head couplers ( $k$ ). For both cases the results are illustrated in Figs. 3(a) and 3(b), respectively ( $\gamma = \gamma_1 = 0.02$ ,  $g = 1$ ,  $r_1 = r_2 = 1$ ,  $L = 1097$  m; for convenience we take  $\beta\Psi_{\text{MZ}} = \beta\Psi_{\text{MI}} = 1$ ). For both cases, the maximum difference between peaks and valleys occurs for a  $k$  value of 0.5. This difference between the peaks and valleys is important because it is directly related to the sensitivity and measurement range of the sensor.

Figures 4(a) and 4(b) show, in more detail, the transfer function versus the modulating frequency for the Mach-Zehnder and Michelson configurations respectively, when the optimum value for  $k$  is chosen. As can be observed, these pictures are two slices of the previous graphs (Fig. 3) at the point  $k = 0.5$ . In Fig. 4(a) the frequencies corresponding to the first valley and to the first constructive interference peak are 94.5 and 189 kHz, respectively, while in Fig. 4(b) they are 47.25 and 94.5 kHz. Although the length of the interferometric fiber structures is the same in both



(a)



(b)

**Fig. 4** Transfer function for the Mach-Zehnder (a) and Michelson (b) configurations ( $k=0.5$ ,  $g=1$ ).

cases, the light in the Michelson topology travels twice along the same path and therefore accumulates a delay time that doubles the one connected with the Mach-Zehnder topology.

These values of the valley and peak frequencies are inversely proportional to the fiber length of the interferometer. In general, it is desirable to have a limited fiber length for these structures, which in turn requires a large modulation frequency, which however is not demanding in system bandwidth, considering that the sinusoidal modulation employed does not introduce higher harmonics than the fundamental. For example, for a fiber length of 50 m in the Michelson topology, the first constructive interference peak occurs at a modulation frequency of 2.073 MHz. The reason for selecting the fiber length of 1097 m for the simulation results presented in this section was merely that was the length of fiber in a coil available in the laboratory.

### 3.2 Measurement Parameter

In this section the behavior of the sensing structures is analyzed further. It is clearly important to know, for each of the proposed configurations, what are the best values for the off-constructive-interference frequency and for the coupling coefficient of the couplers in order to optimize the sensitivity and linearity of the sensors.

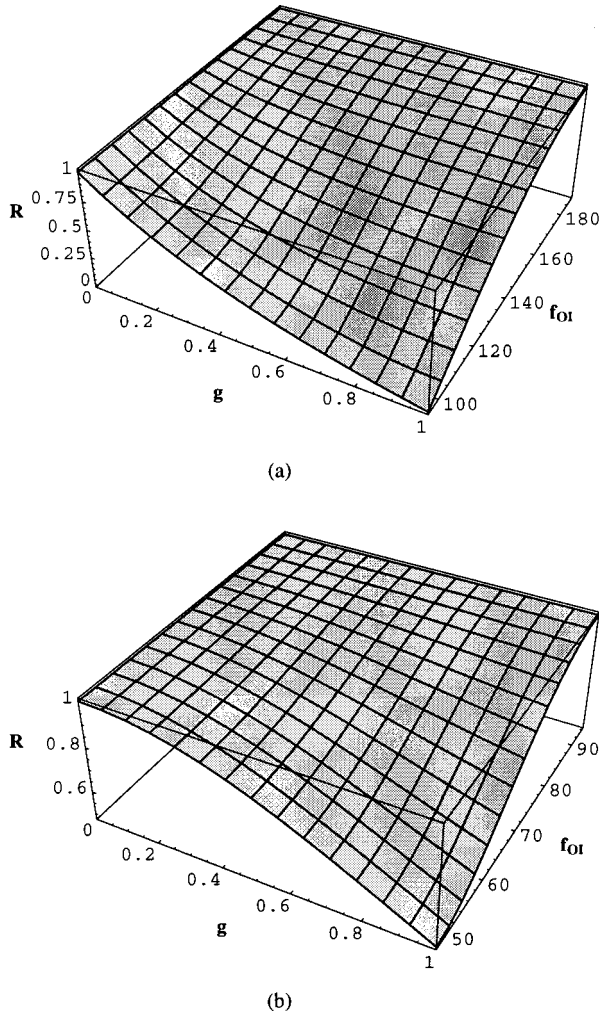


**Fig. 5** Measurement parameter for the Mach-Zehnder (a) and Michelson (b) configurations versus the induced loss factor  $g$  and the off-constructive-interference frequency ( $k=0.5$ ).

The sensing concept is based on the definition of the following parameter, hereafter referred as the *measurement parameter*:

$$R \equiv \frac{V_{0I}}{V_I} \quad (6)$$

where  $V_{0I}$  and  $V_I$  are the values of the system transfer function, respectively, at an off-constructive-interference and at a constructive-interference frequency (Fig. 1). Figures 5(a) and 5(b) show this parameter for the Mach-Zehnder and Michelson structures, respectively, with two variables, namely the induced loss factor ( $g$ ) and the off-constructive-interference frequency. The loss factor was varied from 0 to 1, while the off-constructive-interference frequency was varied from the value corresponding to the first valley up to the one associated with the first constructive-interference peak; the other parameters had the values stated before. As can be observed, for both cases the parameter  $R$  approaches unity in two regions. One of them is where  $g=0$  (no light in one of the interferometer arms), the transfer function being constant for all frequencies, i.e.,

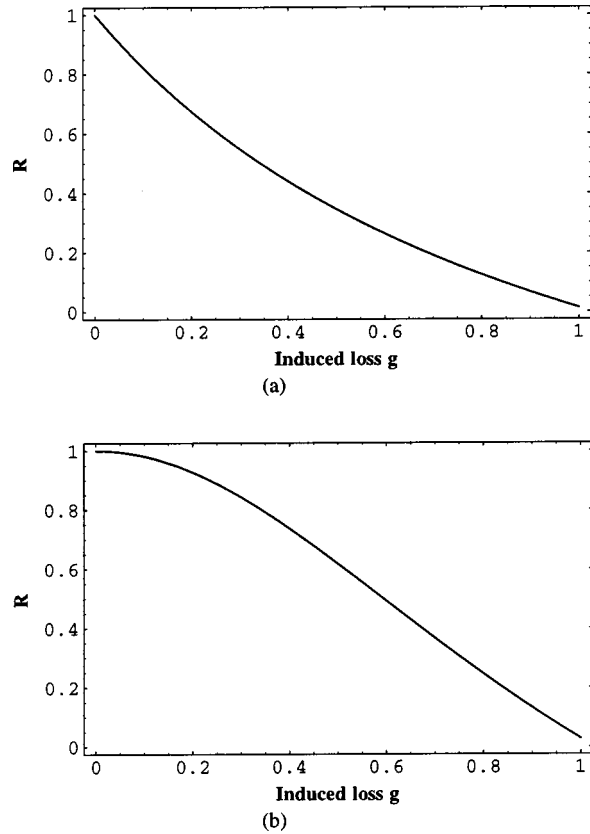
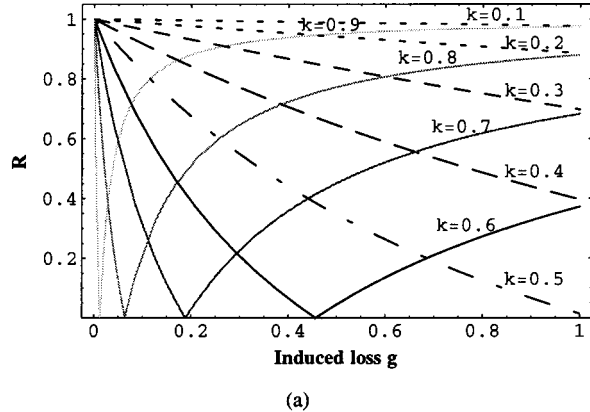


**Fig. 6** Parameter  $R$  for the Mach-Zehnder (a) and Michelson (b) configurations versus the induced optical power loss factor  $g$ . The off-constructive-interference frequencies are the valley frequencies, and  $k=0.5$ .

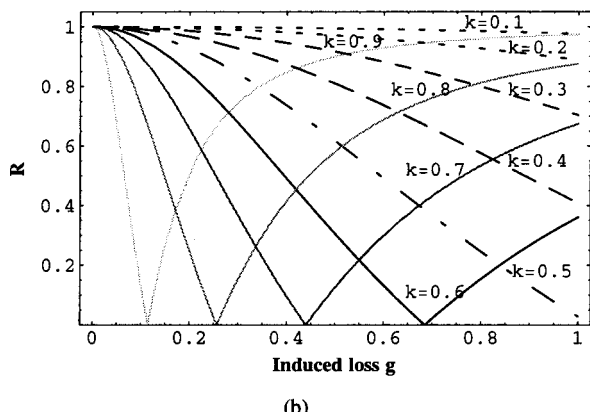
$R=1$ . The other region is where the off-constructive-interference frequency approaches the constructive-interference value (189 and 94.5 kHz for the Mach-Zehnder and Michelson configurations, respectively).

The freedom to choose the off-constructive-interference frequency allows sensor optimization in order to reach an optimum compromise between sensor sensitivity and linearity. In fact, for both topologies, the optimum value for the off-constructive-interference frequency was found to be the valley frequency (94.5 kHz for the Mach-Zehnder and 47.25 kHz for the Michelson). For this situation, Figs. 6(a) and 6(b) show the measurement functions for the Mach-Zehnder and Michelson structures, respectively. With respect to sensor measurement linearity the Michelson configuration is more favorable than the Mach-Zehnder one. This can be quantified by the relative error between the curves and the straight lines that fit them best. It can also be observed that both configurations are able to address the full range of  $R$  values.

Figures 7(a) and 7(b) present the parameter  $R$  for the off-constructive-interference frequency equal to the valley frequency, considering different values of the coupling coefficient ( $k$  being varied from 0.1 to 0.9). It is assumed that the intrinsic losses of the Mach-Zehnder and Michelson topologies can be neglected. From the data presented in these figures, different values for  $k$  can be chosen, according to the required compromise between sensor sensitivity and linearity. However, in general it can be stated that the



(a)



(b)

**Fig. 7** Parameter  $R$  for the Mach-Zehnder (a) and Michelson (b) configurations versus the induced optical power loss factor for several values of  $k$ , taking the off-constructive-interference frequencies to be the valley frequencies.

choice of  $k=0.5$  is an appropriate one, particularly for the Michelson configuration.

#### 4 Experiment

To demonstrate the sensing concept described above, the experimental arrangements shown in Figs. 8(a) (Mach-Zehnder topology) and 8(b) (Michelson topology) were implemented. Two sinusoidal electrical signals with different frequencies were superimposed on the bias current of the light source (edge-emitting LED, Fiber Tech T7503) emitting at 850 nm. Multimode fiber and couplers (100 and 140  $\mu\text{m}$ ) were used. The coupling ratio and the excess loss of the couplers were respectively  $k_1=k_2=0.5$  and  $\gamma_1=\gamma_2=0.056$ , respectively. The path imbalance of the two arms in the Mach-Zehnder and Michelson topologies was the same and approximately 1097 m. In combination with the fiber refractive index, this corresponds to first constructive-interference peak frequencies of 189 and 94.5 kHz for the Mach-Zehnder and Michelson structures, respectively. The reflectivities of the fiber ends were rendered  $\approx 100\%$  by means of an appropriate silvering technique. A variable optical power loss was induced in the arm of the interferometer with lower intrinsic loss in order to balance the optical power in the two arms, thereby optimizing the modulation depth (the visibility). In order to observe the sensor transfer function, one of the electrical signals was turned off and the frequency of the other was swept. To obtain the value of  $R$ , two bandpass filters centered at the frequencies of the sine waves that modulated the injection current of the optical source were used, and the rms values of the corresponding output voltage signals, which are proportional to their amplitudes, were measured. In order to compare the experimentally obtained values for  $R$  with the ones predicted by

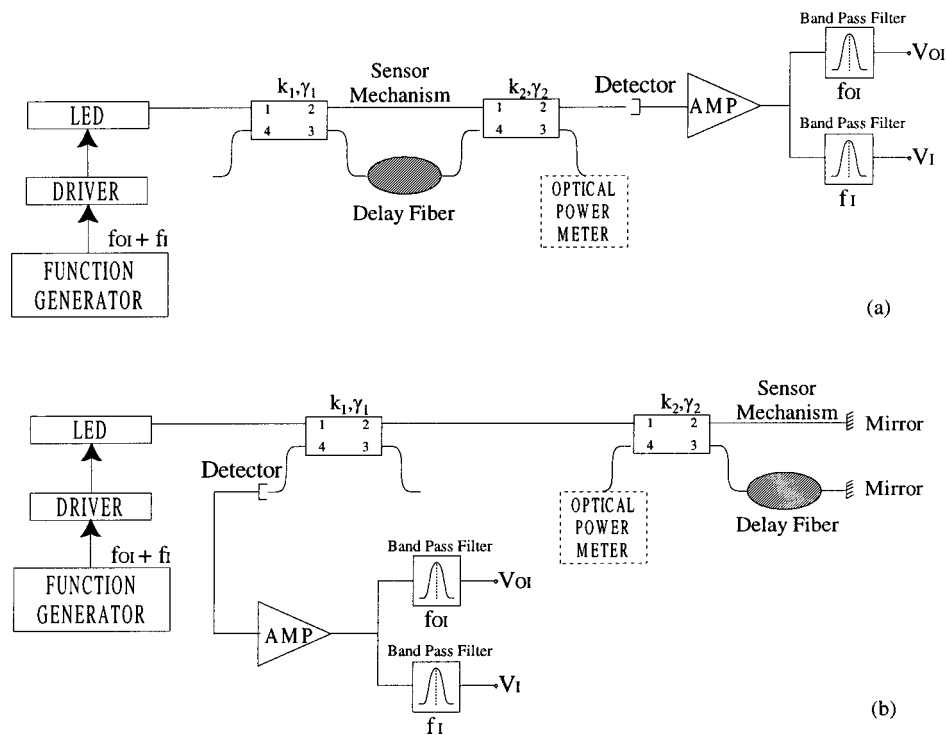


**Fig. 8** Experimental setup for the Mach-Zehnder (a) and Michelson (b) configurations.

the theory it was necessary to know the induced optical power loss factor  $g$ . This was done by applying the following methodology. Considering the Mach-Zehnder sensing structure [Fig. 8(a)], if  $I_{\text{out}}$  is the optical power at port 3 of coupler 2 (measured directly by the optical power meter),  $I_{\text{in}}$  is the optical power at port 1 of coupler 1,  $h_2$  represents the intrinsic losses in the longer arm due to splices and light propagation attenuation in the 1097-m fiber length,  $h_1$  is the loss imposed in the shorter arm in order to have the same amount of optical power in both arms when the induced loss factor equals one (i.e., no induced loss), then the output optical power can be written as

$$\begin{aligned} I_{\text{out}} = & (1 - \gamma_1)(1 - \gamma_2)(1 - k_1)k_2 h_1 g I_{\text{in}} \\ & + (1 - \gamma_1)(1 - \gamma_2)k_1(1 - k_2)h_2 I_{\text{in}}. \end{aligned} \quad (7)$$

Considering now the Michelson sensing structure, if  $h_4$  represents the intrinsic losses in the longer arm due to splices, due to light propagation attenuation in the  $2 \times 1097$ -m fiber length, and due to the fiber end reflectivity coefficients being smaller than one, and if  $h_3$  is the loss imposed in the smaller arm in order to have the same amount of optical power in both arms when  $g = 1$ , then

$$\begin{aligned} I_{\text{out}} = & (1 - \gamma_1)(1 - \gamma_2)^2(1 - k_1)(1 - k_2)k_2 h_3 g^2 I_{\text{in}} \\ & + (1 - \gamma_1)(1 - \gamma_2)^2(1 - k_1)k_2(1 - k_2)h_4 I_{\text{in}}. \end{aligned} \quad (8)$$

For  $g = 0$ , i.e., in the situation when there is no light in the shorter arm of the interferometers, if we substitute in Eqs. (7) and (8) the values for the parameters  $\gamma_1$ ,  $\gamma_2$ ,  $k_1$ , and  $k_2$ , then  $h_2$  and  $h_4$  can be determined, assuming  $I_{\text{in}}$  is known and constant throughout the experiment and  $I_{\text{out}}$  is obtained by the measurement performed by the optical power meter. Naturally, in a real system  $I_{\text{in}}$  will not be constant, but any effect of its fluctuations will be eliminated by the self-referencing properties of the sensing concept described in this work. In the present context  $I_{\text{in}}$  needs to be constant only for the purpose of comparison of the experimental and theoretical results. From the definition of  $h_1$  and  $h_3$  it turns out from Eqs. (7) and (8) that

$$h_1 = \frac{(1 - \gamma_1)(1 - \gamma_2)k_1(1 - k_2)h_2}{(1 - \gamma_1)(1 - \gamma_2)(1 - k_1)k_2}, \quad (9)$$

$$h_3 = \frac{(1 - \gamma_1)(1 - \gamma_2)^2(1 - k_1)k_2(1 - k_2)h_4}{(1 - \gamma_1)(1 - \gamma_2)^2(1 - k_1)(1 - k_2)k_2}. \quad (10)$$

The knowledge of the quantities  $h_1$ ,  $h_2$ ,  $h_3$ ,  $h_4$ , and  $I_{\text{in}}$  permits the determination of the induced optical power loss  $g$  from the measurement of  $I_{\text{out}}$ .

## 5 Results

Figures 9(a) and 9(b) show the experimentally determined sensor transfer functions for the Mach-Zehnder and Michelson configurations, respectively. It was found that they were modulated by the frequency response of the detection and amplification block, which exhibited an evident second-order behavior responsible for the spike in its transfer function just before its  $-3$  dB point, which occurred

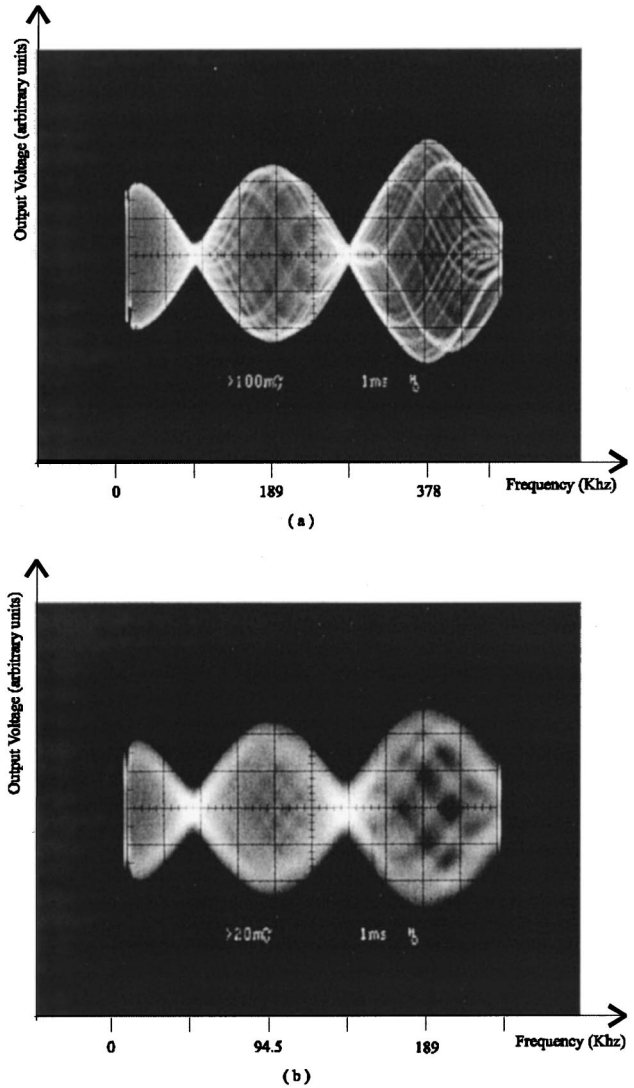


**Fig. 9** Experimental obtained transfer functions for the Mach-Zehnder (a) and Michelson (b) sensing structures.

around 800 kHz. This explains why the amplitudes of the output voltage sinusoidal waveforms at adjacent constructive-interference frequencies are different.

Figures 10(a) and 10(b) plot the results obtained for the parameter  $R$  for the two configurations, when the off-constructive-interference frequency was set to the frequency of the first valley (94.5 and 47.25 kHz for the Mach-Zehnder and Michelson structures, respectively). The values experimentally determined for  $h_2$  and  $h_4$  were  $h_2 = 0.47$  and  $h_4 = 0.30$ . The theoretical curves were obtained using Eqs. (4), (5), and (6), starting from the point where the optical power in the two interferometer arms was balanced and deducing from it the loss parameter  $g$ .

## 6 Discussion

Comparing the results presented in Secs. 3 and 5, it can be stated that they are globally in fairly good agreement, particularly if the lateral shift between the theoretical and experimental results is not valorized. To do so seems reasonable considering that it is the agreement between the slopes

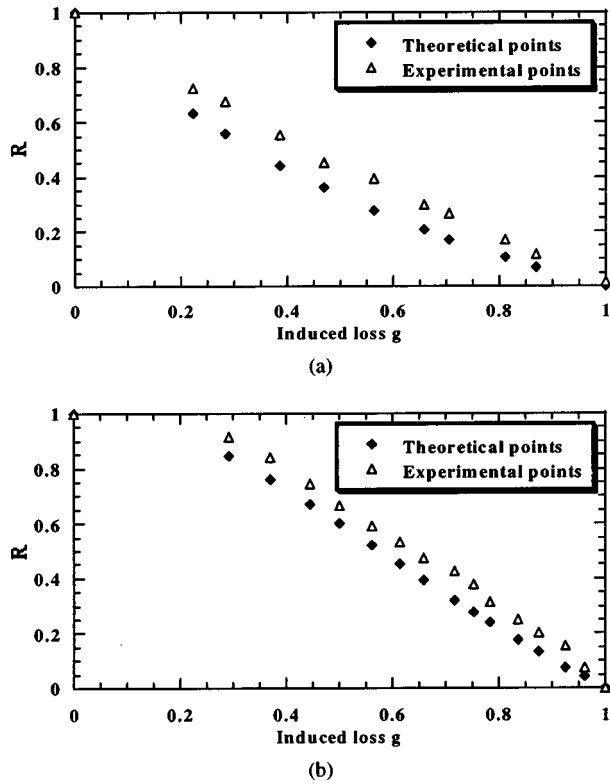


**Fig. 10** Experimental and theoretical results for the measurement parameter for the Mach-Zehnder (a) and the Michelson (b) sensing structures.

of the two sets of data that is crucial to system design. The origin of the lateral shift is under investigation.

The two sensors reveal good sensitivity, a characteristic particularly relevant for monitoring dynamic parameters (e.g., vibration), which do not normally have large amplitudes and consequently produce small induced losses. It must be emphasized that the sensitivity to a given measurand depends not only on the primary sensitivity of the sensing structure, but also on the interface between the measuring and action and the optical loss induced in the sensor head. This is clearly a problem to be addressed in each particular case. It is important to keep in mind that the attainable system resolution is not only determined by the global system sensitivity to the action of a given measurand, but also by the noise level at the system output, these being the two factors that determine the sensor signal-to-noise ratio. The sensing concept described in this work is particularly favorable with regard to the minimization of system noise, because what is monitored is the amplitudes of two sine waves, so that the detection bandwidth can be made as narrow as practically feasible, with consequent decrease of the system noise level.

The sensors' measurement range can be increased by reducing the intrinsic optical losses in the sensing structures (losses in couplers, splices, fiber, etc.). The two most effective ways of doing so are to tailor the sensor operation to longer wavelengths and to reduce the length of the delay fiber. For example, operating with the same multimode fiber at 1300 nm has the potential of reducing the fiber loss by a factor of approximately 8 relative to operation at 830

nm. On the other hand, reducing the length of the delay fiber by a factor of 10 or 20 results in a substantial decrease of the intrinsic optical losses—at the cost, however, of working with higher frequencies (on the order of megahertz).

In respect to linearity, the Michelson configuration presents a better result than the Mach-Zehnder one. Moreover, in the Michelson scheme the emission and detection block plus processing electronics can be located in the same region while the sensing structure can be located remotely. This feature makes the Michelson configuration more attractive in practice.

The sensing configurations described in this work are versatile structures for monitoring static and dynamic physical parameters, requiring a small number of optical components and simple signal processing. Of significant importance is the underlying concept of self-referencing, which essentially solves the problem of compensating optical power fluctuations along the optical system.

In conclusion, in this paper we have described a concept of self-referencing intensity-based optical fiber sensors and applied it to the Mach-Zehnder and Michelson sensing configurations, which we have investigated both theoretically and experimentally. The model developed has proved to be effective in describing the sensor properties, which indicates its usefulness for sensor design and optimization.

## References

1. J. P. Dakin and B. Culshaw, Eds., *Optical Fiber Sensors: Applications, Analysis and Future Trends*, Artech House, London (1997).
2. G. Murtaza and J. M. Senior, "Referenced intensity-based optical fibre sensors," *Int. J. Optoelectron.* **9**(4), 339–348 (1994).
3. G. Adamovsky, "Fiber-optic displacement sensor with temporally separated signals and reference channel," *Appl. Opt.* **27**(7), 1313–1315 (1988).
4. G. Murtaza and J. M. Senior, "Methods for providing stable optical signals in dual wavelength referenced LED based sensors," *IEEE Photonics Technol. Lett.* **6**(8), 1020–1022 (1994).
5. R. I. MacDonald and R. Nychka, "Differential measurement technique for optical fibre sensors," *Electron. Lett.* **27**(23), 2194–2196 (1991).
6. D. N. Davies, J. Chaimowicz, G. Economou, and J. Foley, "Displacement sensor using a compensated fiber link," in *Proc. 2nd Conf. Optical Fiber Sensors*, pp. 387–391, Stuttgart, Germany (1984).
7. P. Sixt, G. Kotrotsios, L. Falco, and O. Parriaux, "Passive fiber Fabry-Perot filter for intensity-modulated sensors referencing," *J. Lightwave Technol.* **4**(7), 926–932 (1986).
8. J. M. Baptista, P. M. Cavaleiro, and J. L. Santos, "Self-referencing intensity based Q-type fibre optic sensor," *Int. J. Optoelectron.* **10**(2), 105–113 (1995).
9. J. M. Baptista, P. M. Cavaleiro, and J. L. Santos, "Self-referencing resonant fiber optic intensity sensor based on a Mach-Zehnder topology," *Rev. Sci. Instrum.* **67**(11), 3788–3794 (1996).



**José M. Baptista** graduated in electrical and computer engineering (telecommunications and computers) from the University of Porto (1991). He received the MSc in physics of laser communications from the University of Essex, Colchester, England (1992). Currently he is teaching in the Polytechnical Institute of Porto, is a researcher in the Optoelectronics Unit at INESC in Porto, and is working towards his PhD degree in the Department of Electrical and Computer Engineering at the University of Porto. He has been publishing papers in the area of fiber optic sensors. He is a member of SPIE and IEEE.



**José L. Santos** graduated in applied physics (optics and electronics) from the University of Porto (1983). He received a PhD from the same university in 1993 in the area of fiber optic sensors. He has the position of assistant professor in the Physics Department of University of Porto, and is the manager of the Optoelectronics Unit at INESC in Porto. Since 1987 his research interests have been in the area of fiber optic sensors. He is a member of SPIE and OSA.



**Armindo S. Lage** graduated in electrical and computer engineering (telecommunications and computers) from the University of Porto (1973). He received a PhD from the same university in the area of optics. He is an assistant professor in the Department of Electrical and Computer Engineering, a researcher in the Faculty of Engineering at the University of Porto, and also a researcher at Centro CIM of Porto. Since 1979 his research interests have included optical metrology and signal processing. He is a member of SPIE.